

## SOBOLEV LVG ANALYSIS OF AMINOMETHANOL AND N-METHYLHYDROXYLAMINE: POTENTIAL SPECTRAL LINES FOR THEIR DETECTION IN A COSMIC OBJECT

M.K.SHARMA<sup>1</sup>, S.CHANDRA<sup>2</sup>

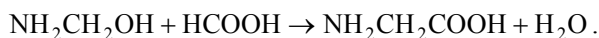
Received 9 June 2021

Accepted 28 July 2021

Aminomethanol ( $\text{NH}_2\text{CH}_2\text{OH}$ ) and N-Methylhydroxylamine ( $\text{CH}_3\text{NHOH}$ ) are isomers of each other, and have astrochemical importance. To our knowledge, they have not been analyzed so far in any terrestrial laboratory, and probably due to non-availability of accurate frequencies, they have not been searched in a cosmic object. It is well known that physical conditions in cosmic objects are very different as compared to those in our terrestrial laboratories. Therefore, these molecules may exist in the interstellar medium. For having information about the potential spectral lines of these molecules, we have obtained their rotational and centrifugal distortion constants, and electric dipole moment with the help of the GAUSSIAN software using B3LYP method, and aug-cc-pVDZ and aug-cc-pVTZ basis sets, separately. As the electric dipole moment has comparable components along all the three  $a$ ,  $b$  and  $c$  axes, we have considered all the three types of radiative transitions together, and have calculated radiative transition probabilities for all the three kinds of radiative transitions. Considering  $a$ ,  $b$  and  $c$  type transitions together, we have performed Sobolev LVG analysis of each molecule, where the collisional rate coefficients have been obtained using a scaling law. Considering energy levels up to  $300\text{ cm}^{-1}$ , we have found 181 weak MASER lines and 112 anomalous absorption transitions of  $\text{NH}_2\text{CH}_2\text{OH}$ , and 21 weak MASER lines and 28 anomalous absorption transitions of  $\text{CH}_3\text{NHOH}$ , which may play important role for the identification of respective molecule in the ISM.

Keywords: *ISM: molecules: aminomethanol: radiative transfer*

1. *Introduction.* Aminomethanol ( $\text{NH}_2\text{CH}_2\text{OH}$ ) and N-Methylhydroxylamine ( $\text{CH}_3\text{NHOH}$ ) are isomers of each other, and have astrochemical importance. ( $\text{NH}_2\text{CH}_2\text{OH}$ ) is considered a precursor of Glycine ( $\text{NH}_2\text{CH}_2\text{COOH}$ ), which is the simplest amino acid:



As  $\text{NH}_2\text{CH}_2\text{OH}$  has been found unstable under normal conditions in terrestrial laboratories, in spite of its importance in the context of the search of life in the universe, its spectrum has not been recorded in the terrestrial laboratories to date. N-methylhydroxylamine ( $\text{CH}_3\text{NHOH}$ ) and its isomeric form Methoxyamine ( $\text{CH}_3\text{ONH}_2$ ) may be considered as a potential interstellar amines [1]. To our knowledge,  $\text{CH}_3\text{NHOH}$  also has not been analyzed in a terrestrial laboratory. In absence of accurate frequencies, probably, attempts have not been made for their search in the interstellar medium (ISM). Hays & Widicus Weaver [2] and McCabe

et al. [3] have performed theoretical study of  $\text{NH}_2\text{CH}_2\text{OH}$ . Hays & Widicus Weaver [2] have reported the rotational constants ( $A$ ,  $B$ ,  $C$ ) and components of electric dipole moment, given in column 4 of Table 1.

For optimization of each of  $\text{NH}_2\text{CH}_2\text{OH}$  and of  $\text{CH}_3\text{NHOH}$  with GAUSSIAN, we have used the Becke three parameter hybrid functional in conjunction with the Lee-Yang-Parr non-local correlation functional (B3LYP) [4,5] method along with the aug-cc-pVDZ and aug-cc-pVTZ basis sets. The values obtained for the rotational and centrifugal distortion constants, in the Watson A-reduced Hamiltonian written in the  $I'$  representation, and the components of electric dipole moment have been given in Table 1. The basis set aug-cc-pVTZ is quite large and consumes large computer-time as compared the basis set aug-cc-pVDZ. However to check the consistency of results, the calculations have been done for two sets. The coordinates of constituent atoms of  $\text{NH}_2\text{CH}_2\text{OH}$  and of  $\text{CH}_3\text{NHOH}$  obtained with the basis set aug-cc-pVTZ are given in Tables 2 and 3, respectively. For identification of  $X$ ,  $Y$ ,  $Z$  components of electric dipole moment in terms of  $\mu_a$ ,  $\mu_b$ ,  $\mu_c$ , we have calculated moments of inertia of aminomethanol and of

Table 1

ROTATIONAL AND CENTRIFUGAL DISTORTION CONSTANTS IN  
MHZ AND ELECTRIC DIPOLE MOMENT COMPONENTS IN DEBYE  
OF  $\text{NH}_2\text{CH}_2\text{OH}$  AND OF  $\text{CH}_3\text{NHOH}$

Constant	$\text{NH}_2\text{CH}_2\text{OH}$			$\text{CH}_3\text{NHOH}$	
	B3LYP/ aug-cc-pVDZ	B3LYP/ aug-cc-pVTZ	Hays and Widicus Weaver	B3LYP/ aug-cc-pVTZ	B3LYP/ aug-cc-pVTZ
A	38484.3503	38829.3069	38693.0	39307.8127	39604.4536
B	9411.5426	9453.9971	9545.7	9851.4694	9870.2923
C	8482.1350	8522.3796	8586.8	8653.3252	8672.9549
$D_J \times 10^3$	9.038281	9.019115		9.647921	9.716917
$D_{JK} \times 10^2$	-3.3238103	-3.2582476		-3.2941772	-3.3115148
$D_K \times 10^1$	3.33572695	3.36754517		3.89720888	4.01392810
$d_1 \times 10^3$	1.653669	1.628417		1.868692	1.867868
$d_2 \times 10^2$	1.1881636	1.1650980		0.0580435	0.0938006
$H_J \times 10^8$	1.306582965	1.343530468		1.166887787	1.128408213
$H_{JK} \times 10^6$	-2.90065885	-3.077371138		-2.817674791	-2.983190456
$H_{KJ} \times 10^6$	8.212567385	8.202668110		10.74020660	11.26734731
$H_K \times 10^8$	7.878483073	8.459248674		-23.60436483	-22.07722507
$h_1 \times 10^9$	8.744733497	9.107103781		7.164633503	6.932223056
$h_2 \times 10^7$	1.541016396	1.780272659		1.516783980	1.391182870
$h_3 \times 10^6$	8.364349985	7.706858871		4.040672955	4.560181498
$\mu_a$ (Debye)	-0.4352	-0.4478	-0.3773	-0.5902	-0.6083
$\mu_b$ (Debye)	-0.9650	-0.9607	-0.9132	0.4226	0.4137
$\mu_c$ (Debye)	1.2404	1.2443	-1.3979	-0.1094	-0.1298

Table 2

STRUCTURE OF NH<sub>2</sub>CH<sub>2</sub>OH MOLECULE

Atom	Coordinates (Å)		
	<i>x</i>	<i>y</i>	<i>z</i>
N	-1.227724	-0.161560	-0.018265
H	-1.374985	-0.780167	0.768468
H	-1.315542	-0.695817	-0.873083
C	0.026844	0.534102	0.047948
H	0.069050	1.075143	0.996231
H	0.073340	1.254711	-0.766122
O	1.207407	-0.263219	-0.117841
H	1.321885	-0.821810	0.657400

N-methylhydroxylamine about the *x*, *y*, *z* axes, using the coordinates given in Tables 2 and 3 as

$$I_x = \sum_i m_i (y_i^2 + z_i^2) I_y = \sum_i m_i (z_i^2 + x_i^2) I_z = \sum_i m_i (x_i^2 + y_i^2) \quad (1)$$

and have considered the convention in molecular physics that  $I_a \leq I_b \leq I_c$ .

Since all the three components of electric dipole moment are comparable to each other, we have calculated energies of rotational levels and radiative transition probabilities for *a*, *b* and *c* type radiative transitions between the levels with the help of the software ASROT [6], where rotational and centrifugal distortion constants, and components of electric dipole moment, given in columns 3 and 5 of Table 1, have been used. The sign of the component of electric dipole moment does not matter, as the square of the component is used in the calculations. These radiative transition probabilities in conjunction with the scaled values of collisional rate coefficients have been utilized in the Sobolev LVG

Table 3

STRUCTURE OF CH<sub>3</sub>NHOH MOLECULE

Atom	Coordinates (Å)		
	<i>x</i>	<i>y</i>	<i>z</i>
C	0.038869	0.536984	0.015667
H	1.219780	-0.240432	0.054413
H	-1.131280	-0.313663	-0.052058
H	0.022913	1.189456	-0.863276
N	-1.384797	-0.693371	0.849931
H	-1.930329	0.162967	-0.445099
O	1.126940	-0.926225	-0.615506
H	0.092775	1.164374	0.909045

analysis of each of the  $\text{NH}_2\text{CH}_2\text{OH}$  and  $\text{CH}_3\text{NHOH}$ . We have found 181 weak MASERs and 112 anomalous absorption transitions of  $\text{NH}_2\text{CH}_2\text{OH}$ , and 21 weak MASERs and 28 anomalous absorption transitions of  $\text{CH}_3\text{NHOH}$ , which may play important role for the identification of respective molecule in the ISM.

2. *Rotational levels.* We have concern only with the rotational levels in the ground vibrational state because the kinetic temperature in a molecular region where Aminomethanol and/or N-Methylhydroxylamine may be found may be few tens of Kelvin (we have considered kinetic temperature up to 50 K). Rotational levels are connected through radiative as well as collisional transitions.

2.1. *Molecular symmetries.* We have considered all the  $a$ ,  $b$  and  $c$  type transitions together. According to the selection rules, for  $a$ -type transitions, the rotational levels can be grouped in two parts:

$$\begin{aligned} k_a, k_c : \quad & \text{odd, odd} \leftrightarrow \text{odd, even} \quad (\text{Group I}) \\ & \text{even, odd} \leftrightarrow \text{even, even} \quad (\text{Group II}). \end{aligned}$$

In Group I, the  $k_a$  is an odd integer whereas in Group II, the  $k_a$  is an even integer. There are neither optical nor collisional transitions between the levels of Group I and of Group II.

According to the selection rules, for the  $b$ -type transitions, the rotational levels are also grouped in two parts:

$$\begin{aligned} k_a, k_c : \quad & \text{even, odd} \leftrightarrow \text{odd, even} \quad (\text{Group III}) \\ & \text{even, even} \leftrightarrow \text{odd, odd} \quad (\text{Group IV}). \end{aligned}$$

In Group III, the  $(k_a + k_c)$  is an odd integer whereas in Group IV, the  $(k_a + k_c)$  is an even integer. Here, also, there are neither optical nor collisional transitions between the levels of Group III and of Group IV.

According to the selection rules, for the  $c$ -type transitions, the rotational levels can be grouped in two parts:

$$\begin{aligned} k_a, k_c : \quad & \text{odd, odd} \leftrightarrow \text{even, odd} \quad (\text{Group V}) \\ & \text{odd, even} \leftrightarrow \text{even, even} \quad (\text{Group VI}). \end{aligned}$$

In Group V, the  $k_c$  is an odd integer whereas in Group VI, the  $k_c$  is an even integer. Here, also, there are neither optical nor collisional transitions between the levels of Group V and of Group VI.

Besides the above selection rules, for the radiative transitions, for each group, there is additional selection rule for the rotational quantum number  $J$ :  $\Delta J = 0, \pm 1$ .

2.2. *Radiative transitions.* The radiative transitions between the rotational levels follow some selection rules, as given above, depending on the direction of the component of electric dipole moment. In our investigation, we have considered

all  $a$ ,  $b$  and  $c$  type radiative transitions, together. We have considered lower 300 rotational levels, having energy up to  $153.91 \text{ cm}^{-1}$  for NH<sub>2</sub>CH<sub>2</sub>OH, and up to  $157.25 \text{ cm}^{-1}$  for CH<sub>3</sub>NHOH. These levels have 3963 radiative transitions for NH<sub>2</sub>CH<sub>2</sub>OH and 4061 radiative transitions for CH<sub>3</sub>NHOH. 29 pairs of NH<sub>2</sub>CH<sub>2</sub>OH, and 23 pairs of CH<sub>3</sub>NHOH of rotational levels have been found to have equal energies. So, we have not considered any kind of transitions between the levels of these pairs.

Using rotational and centrifugal distortion constants, and components of electric dipole moment, we have calculated energies of rotational levels and Einstein  $A$ -coefficients of rotational transitions with the help of the software ASROT [6]. There are well known relations between the Einstein  $A$  and  $B$  coefficients:

$$A_{ul} = \frac{2h\nu_{ul}^3}{c^2} B_{ul} \quad \text{and} \quad B_{ul} = \frac{g_l}{g_u} B_{lu}, \quad (2)$$

where  $g_u$  and  $g_l$  denote the statistical weights of upper and lower levels, respectively.

**2.3. Collisional transitions.** The rotational levels, besides the radiative transitions, are connected through the collisional transitions, where colliding partner is the H<sub>2</sub> molecule, which is in general the most abundant molecule in the molecular regions. Though the collisional transitions do not follow any selection rules, computation of collisional rate coefficients is difficult part in the study of interstellar molecules [7-9]. Moreover, following the molecular symmetries, the collisional transitions are between the levels within a group [10].

Further, the collisional rate coefficients need to be calculated for one direction (excitation or deexcitation) of transitions, as for the reverse direction, the collisional rate coefficients are calculated with the help of the detailed equilibrium [11]. As the case with these molecules, when collisional rate coefficients are not available, they have been estimated using different scaling laws [12-18]. Here, we have calculated deexcitation rate coefficients with the help of the following relation for a kinetic temperature  $T$  [19,20]:

$$C(J'_{k'_a, k'_c} \rightarrow J_{k_a, k_c}) = \frac{1 \times 10^{-11}}{2J'+1} \sqrt{T}. \quad (3)$$

This expression can be interpreted as the cross-section times the relative velocity between aminomethanol and H<sub>2</sub> molecule. These collisional rate coefficients do not produce any anomalous phenomenon from their own.

**3. Details of model.** So obtained radiative transition probabilities and collisional rate coefficients have been used for solving a set of statistical equilibrium equations coupled with the equations of radiative transfer (Sobolev LVG analysis). Details of the model used in the present work have been discussed [21-26]. The

external radiation field is the CMB only with the background temperature  $T_{bg} = 2.73$  K. In the context of  $\text{CH}_3\text{OH}$  MASER, Nesterenok [26] have discussed that the Sobolev approximation is applicable to limited region.

4. *Results and discussion.* For each molecule, the set of statistical equilibrium equations coupled with the equations of radiative transfer is solved through iteration method, where starting population-densities are the thermal values at given kinetic temperature  $T$ . By solving the set of equations, nonthermal population densities of levels have been obtained as a function of the density of colliding partner,  $n_{H_2}$ , kinetic temperature  $T$ , and parameter  $\gamma = n_{mol}/(dv_r/dr)$ , where  $n_{mol}$  denotes the density of the molecule and  $dv_r/dr$  is the velocity-gradient in the region. In the calculations,  $\gamma$  is taken as a parameter. The  $\gamma$  parameter includes the column density of the molecule of interest.

To make our results applicable to various types of cosmic objects, in the analysis, we have considered wide ranges of physical parameters. The molecular hydrogen density  $n_{H_2}$  is taken from  $10^2$  to  $10^6 \text{ cm}^{-3}$ ; the kinetic temperatures  $T$  are taken 10, 20, 30, 40, 50 K. For  $\gamma$ , we have taken two values as  $10^{-5}$  and  $10^{-6} \text{ cm}^{-3} (\text{km/s})^{-1} \text{ pc}$ .

The radiative life-times of rotational levels have been calculated using the Einstein  $A$ -coefficients. Radiative life-time of upper level  $t_u$  is generally smaller than that of the lower one  $t_l$ . But, the reverse is true for a MASER transition. However, larger life-time of upper level is not a sufficient criterion of MASER action. For the MASER action, population inversion ( $n_u g_l / n_l g_u > 1$ ) between the upper level  $u$  and lower level  $l$  is also required. Here,  $n$  denotes the population density of level. For a radiative transition to be a weak MASER, we have considered two criteria:

1. Radiative life-time of upper level is larger than that of the lower level.
2. There is population inversion between the levels of transition.

In the present investigation, we have taken  $t_u/t_l > 1.2$  and  $n_u g_l / n_l g_u > 1.2$ . We have found 181 weak MASERs of  $\text{NH}_2\text{CH}_2\text{OH}$ , and 21 weak MASERs of  $\text{CH}_3\text{NHOH}$ . Information about 40 transitions between lower levels of  $\text{NH}_2\text{CH}_2\text{OH}$ , and all 31 transitions of  $\text{CH}_3\text{NHOH}$  is given in Tables 4 and 5, respectively, where we have given frequency and Einstein  $A$ -coefficient of transition, energy of upper level, life-times of upper and lower levels. For 7 lines (written on the left) among the lowest levels, the variation of  $n_u g_l / n_l g_u$  versus molecular hydrogen density  $n_{H_2}$  for kinetic temperatures of 10, 20, 30, 40 and 50 K, are given in Fig.1 and 2, respectively. MASER action is in the region where  $n_u g_l / n_l g_u$  is larger than 1. For these 7 lines, the MASER action is found to increase with kinetic temperature. At large densities, the MASER action decreases or diminishes as the collisions destroy the population inversion.

Table 4

FREQUENCY  $\nu$ , EINSTEIN A-COEFFICIENT  $A_{ul}$ , ENERGY  $E_u$  OF UPPER LEVEL, RADIATIVE LIFE-TIME  $t_u$  OF UPPER LEVEL AND  $t_l$  OF LOWER LEVEL FOR 40 WEAK MASER TRANSITIONS BETWEEN LOWER LEVELS OF NH<sub>2</sub>CH<sub>2</sub>OH

Transition	$\nu$ (MHz)	$A_{ul}$ (s <sup>-1</sup> )	$E_u$ (cm <sup>-1</sup> )	$t_u$ (s)	$t_l$ (s)
2 <sub>0,2</sub> -1 <sub>1,0</sub>	5624.035	3.057E-10	1.797	2.28E+07	1.21E+06
2 <sub>0,2</sub> -1 <sub>1,1</sub>	6555.593	3.169E-10	1.797	2.28E+07	1.64E+06
5 <sub>1,4</sub> -4 <sub>2,2</sub>	6876.447	3.583E-10	10.210	9.42E+04	3.28E+04
5 <sub>1,4</sub> -4 <sub>2,3</sub>	7202.637	2.441E-10	10.210	9.42E+04	3.30E+04
6 <sub>1,6</sub> -5 <sub>2,3</sub>	7544.221	2.402E-10	13.241	1.27E+05	2.64E+04
6 <sub>1,6</sub> -5 <sub>2,4</sub>	8302.680	5.746E-10	13.241	1.27E+05	2.66E+04
9 <sub>2,8</sub> -8 <sub>3,5</sub>	10810.444	8.054E-10	30.908	1.17E+04	5.78E+03
9 <sub>2,8</sub> -8 <sub>3,6</sub>	10956.738	1.444E-09	30.908	1.17E+04	5.78E+03
9 <sub>2,7</sub> -8 <sub>3,5</sub>	17643.296	6.222E-09	31.136	1.13E+04	5.78E+03
9 <sub>2,7</sub> -8 <sub>3,6</sub>	17789.591	3.715E-09	31.136	1.13E+04	5.78E+03
7 <sub>1,7</sub> -6 <sub>2,4</sub>	21338.741	5.529E-09	17.318	8.72E+04	2.12E+04
3 <sub>0,3</sub> -2 <sub>1,1</sub>	22580.951	2.735E-08	3.592	4.75E+06	5.44E+05
7 <sub>1,7</sub> -6 <sub>2,5</sub>	22846.783	1.289E-08	17.318	8.72E+04	2.15E+04
3 <sub>0,3</sub> -2 <sub>1,2</sub>	25375.546	2.704E-08	3.592	4.75E+06	9.08E+05
6 <sub>1,5</sub> -5 <sub>2,2</sub>	27074.740	2.703E-08	13.892	6.16E+04	2.64E+04
6 <sub>1,5</sub> -5 <sub>2,4</sub>	27833.199	1.708E-08	13.892	6.16E+04	2.66E+04
8 <sub>1,8</sub> -7 <sub>2,5</sub>	34175.284	2.199E-08	21.974	6.18E+04	1.71E+04
8 <sub>1,8</sub> -7 <sub>2,6</sub>	36865.323	5.636E-08	21.974	6.18E+04	1.74E+04
4 <sub>0,4</sub> -3 <sub>1,2</sub>	38955.140	1.570E-07	5.981	1.40E+06	2.74E+05
4 <sub>0,4</sub> -3 <sub>1,3</sub>	44543.777	1.768E-07	5.981	1.40E+06	5.10E+05
9 <sub>1,9</sub> -8 <sub>2,6</sub>	45926.926	4.968E-08	27.208	4.51E+04	1.39E+04
7 <sub>1,6</sub> -6 <sub>2,4</sub>	47345.829	1.699E-07	18.185	4.23E+04	2.12E+04
7 <sub>1,6</sub> -6 <sub>2,5</sub>	48853.870	1.066E-07	18.185	4.23E+04	2.15E+04
9 <sub>1,9</sub> -8 <sub>2,7</sub>	50352.430	1.462E-07	27.208	4.51E+04	1.42E+04
5 <sub>0,5</sub> -4 <sub>1,3</sub>	54678.589	4.495E-07	8.963	5.55E+05	1.54E+05
10 <sub>1,10</sub> -9 <sub>2,7</sub>	56472.195	8.321E-08	33.018	3.36E+04	1.13E+04
10 <sub>1,10</sub> -9 <sub>2,8</sub>	63305.048	2.913E-07	33.018	3.36E+04	1.17E+04
5 <sub>0,5</sub> -4 <sub>1,4</sub>	63990.764	5.952E-07	8.963	5.55E+05	3.04E+05
8 <sub>1,7</sub> -7 <sub>2,5</sub>	67548.656	5.631E-07	23.086	3.01E+04	1.71E+04
6 <sub>0,6</sub> -5 <sub>1,4</sub>	69672.246	9.231E-07	12.533	2.69E+05	9.42E+04
8 <sub>1,7</sub> -7 <sub>2,6</sub>	70238.695	3.561E-07	23.086	3.01E+04	1.74E+04
6 <sub>0,6</sub> -5 <sub>1,5</sub>	83633.959	1.468E-06	12.533	2.69E+05	1.91E+05
7 <sub>0,7</sub> -6 <sub>1,5</sub>	83851.217	1.553E-06	16.687	1.50E+05	6.16E+04
9 <sub>1,8</sub> -8 <sub>2,6</sub>	87529.776	1.367E-06	28.594	2.21E+04	1.39E+04
9 <sub>1,8</sub> -8 <sub>2,7</sub>	91955.280	8.846E-07	28.594	2.21E+04	1.42E+04
8 <sub>0,8</sub> -7 <sub>1,6</sub>	97132.285	2.282E-06	21.423	9.17E+04	4.23E+04
10 <sub>1,9</sub> -9 <sub>2,7</sub>	107130.744	2.746E-06	34.707	1.67E+04	1.13E+04
9 <sub>0,9</sub> -8 <sub>1,7</sub>	109443.247	3.035E-06	26.734	6.01E+04	3.01E+04
10 <sub>1,9</sub> -9 <sub>2,8</sub>	113963.597	1.848E-06	34.707	1.67E+04	1.17E+04
10 <sub>0,10</sub> -9 <sub>1,8</sub>	120732.692	3.740E-06	32.619	4.15E+04	2.21E+04

Table 5

FREQUENCY  $\nu$ , EINSTEIN A-COEFFICIENT  $A_{ul}$ , ENERGY  $E_u$   
 OF UPPER LEVEL, RADIATIVE LIFE-TIME  $t_u$  OF UPPER LEVEL  
 AND  $t_l$  OF LOWER LEVEL FOR 21 WEAK MASER  
 TRANSITIONS OF NH<sub>3</sub>NHOH

Transition	$\nu$ (MHz)	$A_{ul}$ (s <sup>-1</sup> )	$E_u$ (cm <sup>-1</sup> )	$t_u$ (s)	$t_l$ (s)
8 <sub>2,6</sub> -7 <sub>3,4</sub>	1997.447	8.768E-14	26.498	9.13E+04	6.46E+04
8 <sub>2,6</sub> -7 <sub>3,5</sub>	2134.260	1.076E-12	26.498	9.13E+04	6.46E+04
17 <sub>2,15</sub> -16 <sub>4,12</sub>	5504.152	2.571E-13	100.690	1.22E+04	9.59E+03
5 <sub>1,4</sub> -4 <sub>2,2</sub>	9936.466	1.208E-11	10.573	5.52E+05	3.39E+05
5 <sub>1,4</sub> -4 <sub>2,3</sub>	10465.821	1.429E-10	10.573	5.52E+05	3.37E+05
12 <sub>3,10</sub> -11 <sub>4,7</sub>	11514.904	1.796E-10	57.419	2.39E+04	1.94E+04
12 <sub>3,10</sub> -11 <sub>4,8</sub>	11578.787	1.836E-11	57.419	2.39E+04	1.94E+04
9 <sub>2,8</sub> -8 <sub>3,5</sub>	12325.126	2.176E-10	31.803	6.67E+04	5.27E+04
9 <sub>2,8</sub> -8 <sub>3,6</sub>	12624.821	2.385E-11	31.803	6.67E+04	5.27E+04
12 <sub>3,9</sub> -11 <sub>4,7</sub>	14632.910	3.728E-11	57.523	2.41E+04	1.94E+04
12 <sub>3,9</sub> -11 <sub>4,8</sub>	14696.793	3.759E-10	57.523	2.41E+04	1.94E+04
9 <sub>2,7</sub> -8 <sub>3,5</sub>	23136.013	1.545E-10	32.164	6.88E+04	5.27E+04
9 <sub>2,7</sub> -8 <sub>3,6</sub>	23435.708	1.585E-09	32.164	6.88E+04	5.27E+04
18 <sub>2,16</sub> -17 <sub>4,13</sub>	30549.818	5.424E-11	112.109	1.03E+04	8.41E+03
6 <sub>1,5</sub> -5 <sub>2,3</sub>	31143.245	4.638E-10	14.391	3.17E+05	2.41E+05
6 <sub>1,5</sub> -5 <sub>2,4</sub>	32371.716	5.170E-09	14.391	3.17E+05	2.38E+05
10 <sub>2,8</sub> -9 <sub>3,6</sub>	44914.361	1.257E-09	38.477	5.28E+04	4.30E+04
10 <sub>2,8</sub> -9 <sub>3,7</sub>	45510.112	1.263E-08	38.477	5.28E+04	4.30E+04
13 <sub>10,3</sub> -14 <sub>9,5</sub>	315004.094	7.959E-08	157.253	1.79E+04	2.59E+03
13 <sub>10,3</sub> -13 <sub>9,5</sub>	574861.418	4.592E-06	157.253	1.79E+04	2.70E+03
13 <sub>10,3</sub> -12 <sub>9,3</sub>	816145.845	3.873E-05	157.253	1.79E+04	2.80E+03

At high densities, for a transition, both brightness temperature and excitation temperature tend to the kinetic temperature in the region (thermalization), whereas at low densities, the brightness temperature and excitation temperature both tend to the CMB temperature of 2.73 K. Meaning that the brightness temperature and excitation temperature of an spectral line should not be less than the CMB temperature. But, 112 transitions of NH<sub>2</sub>CH<sub>2</sub>OH, and 28 transitions of CH<sub>3</sub>NHOH have been found to show the excitation temperature less than 2.73 K (anomalous absorption). Information about 40 transitions between lower levels of NH<sub>2</sub>CH<sub>2</sub>OH, and all 28 transitions of CH<sub>3</sub>NHOH is given in Tables 6 and 7, respectively. For 7 lines (written on the left) among the lowest levels, the variation of excitation temperature  $T_{ex}$  versus molecular hydrogen density  $n_{H_2}$  for kinetic temperatures of 10, 20, 30, 40 and 50 K, are given in Fig.3 and 4, respectively. Anomalous absorption is in the region where the excitation temperature is less than 2.73 K. It may be noted that for the transition 2<sub>02</sub>-1<sub>10</sub> of NH<sub>2</sub>CH<sub>2</sub>OH, the radiative life

Table 6

FREQUENCY  $\nu$ , EINSTEIN A-COEFFICIENT  $A_{ul}$ , ENERGY  $E_u$  OF UPPER LEVEL, RADIATIVE LIFE-TIME  $t_u$  OF UPPER LEVEL AND  $t_l$  OF LOWER LEVEL FOR 40 ANOMALOUS ABSORPTION TRANSITIONS BETWEEN LOWER LEVELS OF NH<sub>2</sub>CH<sub>2</sub>OH

Transition	$\nu$ (MHz)	$A_{ul}$ (s <sup>-1</sup> )	$E_u$ (cm <sup>-1</sup> )	$t_u$ (s)	$t_l$ (s)
2 <sub>0,2</sub> -1 <sub>1,0</sub>	5763.225	3.268E-10	1.789	2.44E+07	1.25E+06
4 <sub>2,3</sub> -5 <sub>1,5</sub>	6759.076	3.325E-10	9.970	3.30E+04	1.91E+05
4 <sub>2,2</sub> -5 <sub>1,5</sub>	7085.266	2.226E-10	9.981	3.28E+04	1.91E+05
3 <sub>2,2</sub> -4 <sub>1,3</sub>	13017.161	1.377E-09	7.574	4.05E+04	1.54E+05
3 <sub>2,1</sub> -4 <sub>1,3</sub>	13126.091	2.342E-09	7.578	4.04E+04	1.54E+05
7 <sub>1,7</sub> -7 <sub>0,7</sub>	18916.435	7.310E-08	17.318	8.72E+04	1.50E+05
6 <sub>1,6</sub> -6 <sub>0,6</sub>	21258.068	9.955E-08	13.241	1.27E+05	2.69E+05
3 <sub>2,2</sub> -4 <sub>1,4</sub>	22329.336	9.900E-09	7.574	4.05E+04	3.04E+05
3 <sub>2,1</sub> -4 <sub>1,4</sub>	22438.266	6.013E-09	7.578	4.04E+04	3.04E+05
5 <sub>1,5</sub> -5 <sub>0,5</sub>	23466.787	1.288E-07	9.745	1.91E+05	5.55E+05
4 <sub>1,4</sub> -4 <sub>0,4</sub>	25454.310	1.589E-07	6.830	3.04E+05	1.40E+06
3 <sub>1,3</sub> -3 <sub>0,3</sub>	27142.157	1.871E-07	4.496	5.10E+05	4.75E+06
2 <sub>1,2</sub> -2 <sub>0,2</sub>	28465.483	2.111E-07	2.746	9.08E+05	2.28E+07
1 <sub>1,0</sub> -1 <sub>0,1</sub>	30306.626	1.495E-07	1.609	1.21E+06	2.21E+08
2 <sub>1,1</sub> -2 <sub>0,2</sub>	31260.079	1.615E-07	2.839	5.44E+05	2.28E+07
3 <sub>1,2</sub> -3 <sub>0,3</sub>	32730.795	1.809E-07	4.683	2.74E+05	4.75E+06
2 <sub>2,1</sub> -3 <sub>1,2</sub>	32809.848	1.341E-08	5.776	4.87E+04	2.74E+05
2 <sub>2,0</sub> -3 <sub>1,2</sub>	32831.652	2.199E-08	5.777	4.87E+04	2.74E+05
4 <sub>1,3</sub> -4 <sub>0,4</sub>	34766.485	2.098E-07	7.140	1.54E+05	1.40E+06
5 <sub>1,4</sub> -5 <sub>0,5</sub>	37428.500	2.508E-07	10.210	9.42E+04	5.55E+05
2 <sub>2,1</sub> -3 <sub>1,3</sub>	38398.485	3.207E-08	5.776	4.87E+04	5.10E+05
2 <sub>2,0</sub> -3 <sub>1,3</sub>	38420.289	1.958E-08	5.777	4.87E+04	5.10E+05
5 <sub>3,3</sub> -6 <sub>2,4</sub>	40119.563	3.185E-08	17.944	8.32E+03	2.12E+04
5 <sub>3,2</sub> -6 <sub>2,4</sub>	40128.483	5.264E-08	17.944	8.32E+03	2.12E+04
6 <sub>1,5</sub> -6 <sub>0,6</sub>	40788.587	3.080E-07	13.892	6.16E+04	2.69E+05
5 <sub>3,3</sub> -6 <sub>2,5</sub>	41627.605	5.839E-08	17.944	8.32E+03	2.15E+04
5 <sub>3,2</sub> -6 <sub>2,5</sub>	41636.525	3.537E-08	17.944	8.32E+03	2.15E+04
4 <sub>3,2</sub> -5 <sub>2,3</sub>	58671.296	7.326E-08	14.945	9.26E+03	2.64E+04
4 <sub>3,1</sub> -5 <sub>2,3</sub>	58673.528	1.201E-07	14.946	9.26E+03	2.64E+04
4 <sub>3,2</sub> -5 <sub>2,4</sub>	59429.755	1.244E-07	14.945	9.26E+03	2.66E+04
4 <sub>3,1</sub> -5 <sub>2,4</sub>	59431.987	7.590E-08	14.946	9.26E+03	2.66E+04
3 <sub>3,1</sub> -4 <sub>2,2</sub>	76985.649	8.884E-08	12.547	1.02E+04	3.28E+04
3 <sub>3,0</sub> -4 <sub>2,2</sub>	76985.968	1.448E-07	12.547	1.02E+04	3.28E+04
3 <sub>3,1</sub> -4 <sub>2,3</sub>	77311.839	1.465E-07	12.547	1.02E+04	3.30E+04
3 <sub>3,0</sub> -4 <sub>2,3</sub>	77312.158	8.985E-08	12.547	1.02E+04	3.30E+04
5 <sub>3,2</sub> -6 <sub>0,6</sub>	162345.981	1.045E-08	17.944	8.32E+03	2.69E+05
4 <sub>3,2</sub> -5 <sub>0,6</sub>	179485.889	3.271E-09	14.945	9.26E+03	5.55E+05
4 <sub>3,1</sub> -5 <sub>0,5</sub>	179488.121	5.315E-09	14.946	9.26E+03	5.55E+05
3 <sub>3,1</sub> -4 <sub>0,4</sub>	196982.776	1.009E-09	12.547	1.02E+04	1.40E+06
3 <sub>3,0</sub> -4 <sub>0,4</sub>	196983.095	1.633E-09	12.547	1.02E+04	1.40E+06

Table 7

FREQUENCY  $\nu$ , EINSTEIN A-COEFFICIENT  $A_{ul}$ , ENERGY  $E_u$  OF UPPER LEVEL, RADIATIVE LIFE-TIME  $t_u$  OF UPPER LEVEL AND  $t_l$  OF LOWER LEVEL FOR 28 ANOMALOUS ABSORPTION TRANSITIONS OF  $\text{NH}_3\text{NHOH}$

Transition	$\nu$ (MHz)	$A_{ul}$ ( $\text{s}^{-1}$ )	$E_u$ ( $\text{cm}^{-1}$ )	$t_u$ (s)	$t_l$ (s)
$7_{3.5}-8_{2.7}$	4928.033	1.445E-12	26.427	6.46E+04	8.90E+04
$7_{3.4}-8_{2.7}$	5064.846	1.574E-11	26.431	6.46E+04	8.90E+04
$10_{4.7}-11_{3.8}$	5236.470	1.728E-11	50.216	2.24E+04	2.90E+04
$10_{4.6}-11_{3.8}$	5266.405	1.743E-12	50.217	2.24E+04	2.90E+04
$10_{4.7}-11_{3.9}$	7135.088	4.319E-12	50.216	2.24E+04	2.89E+04
$10_{4.6}-11_{3.9}$	7165.023	4.410E-11	50.217	2.24E+04	2.89E+04
$4_{2.3}-5_{1.5}$	7472.492	4.749E-12	10.224	3.37E+05	4.52E+05
$4_{2.2}-5_{1.5}$	8001.847	5.719E-11	10.242	3.39E+05	4.52E+05
$13_{5.9}-14_{4.10}$	10723.798	1.458E-10	81.593	1.02E+04	1.26E+04
$13_{5.8}-14_{4.10}$	10729.824	1.446E-11	81.593	1.02E+04	1.26E+04
$3_{2.2}-4_{1.3}$	10932.318	1.546E-10	7.753	4.66E+05	1.09E+06
$3_{2.1}-4_{1.3}$	11109.274	1.571E-11	7.759	4.68E+05	1.09E+06
$13_{5.9}-14_{4.11}$	11149.618	1.622E-11	81.593	1.02E+04	1.26E+04
$13_{5.8}-14_{4.11}$	11155.645	1.641E-10	81.593	1.02E+04	1.26E+04
$6_{3.4}-7_{2.5}$	18455.181	6.953E-10	22.092	7.87E+04	1.24E+05
$6_{3.3}-7_{2.5}$	18510.066	6.859E-11	22.093	7.87E+04	1.24E+05
$6_{3.4}-7_{2.6}$	22776.940	1.254E-10	22.092	7.87E+04	1.21E+05
$6_{3.3}-7_{2.6}$	22831.825	1.290E-09	22.093	7.87E+04	1.21E+05
$3_{2.2}-4_{1.4}$	22899.573	1.137E-10	7.753	4.66E+05	8.27E+05
$3_{2.1}-4_{1.4}$	23076.529	1.186E-09	7.759	4.68E+05	8.27E+05
$2_{2.1}-3_{1.2}$	31794.925	2.297E-09	5.899	6.04E+05	2.58E+06
$2_{2.0}-3_{1.2}$	31830.360	2.199E-10	5.900	6.05E+05	2.58E+06
$5_{3.3}-6_{2.4}$	38427.048	5.209E-09	18.377	9.46E+04	1.71E+05
$5_{3.2}-6_{2.4}$	38445.378	5.035E-10	18.378	9.46E+04	1.71E+05
$2_{2.1}-3_{1.3}$	38977.733	3.593E-10	5.899	6.04E+05	1.73E+06
$2_{2.0}-3_{1.3}$	39013.169	3.764E-09	5.900	6.05E+05	1.73E+06
$5_{3.3}-6_{2.5}$	40861.693	5.982E-10	18.377	9.46E+04	1.69E+05
$5_{3.2}-6_{2.5}$	40880.023	6.204E-09	18.378	9.46E+04	1.69E+05

time of upper level is larger than that of lower level, but it shows the anomalous absorption.

We are aware of the fact that in absence of laboratory spectrum, non-availability of accurate frequencies may be a hurdle. However, in a region where other lines are not present, 1% variation of frequency may be considered. We are willing to provide complete list of lines on demand.

5. *Conclusion.* On optimization of  $\text{NH}_2\text{CH}_2\text{OH}$  and of  $\text{CH}_3\text{NHOH}$  with the help of GAUSSIAN, we have obtained rotational and centrifugal distortion

constants, and components of electric dipole moment. For getting information about potential spectral lines of these molecules, we have performed Sobolev LVG

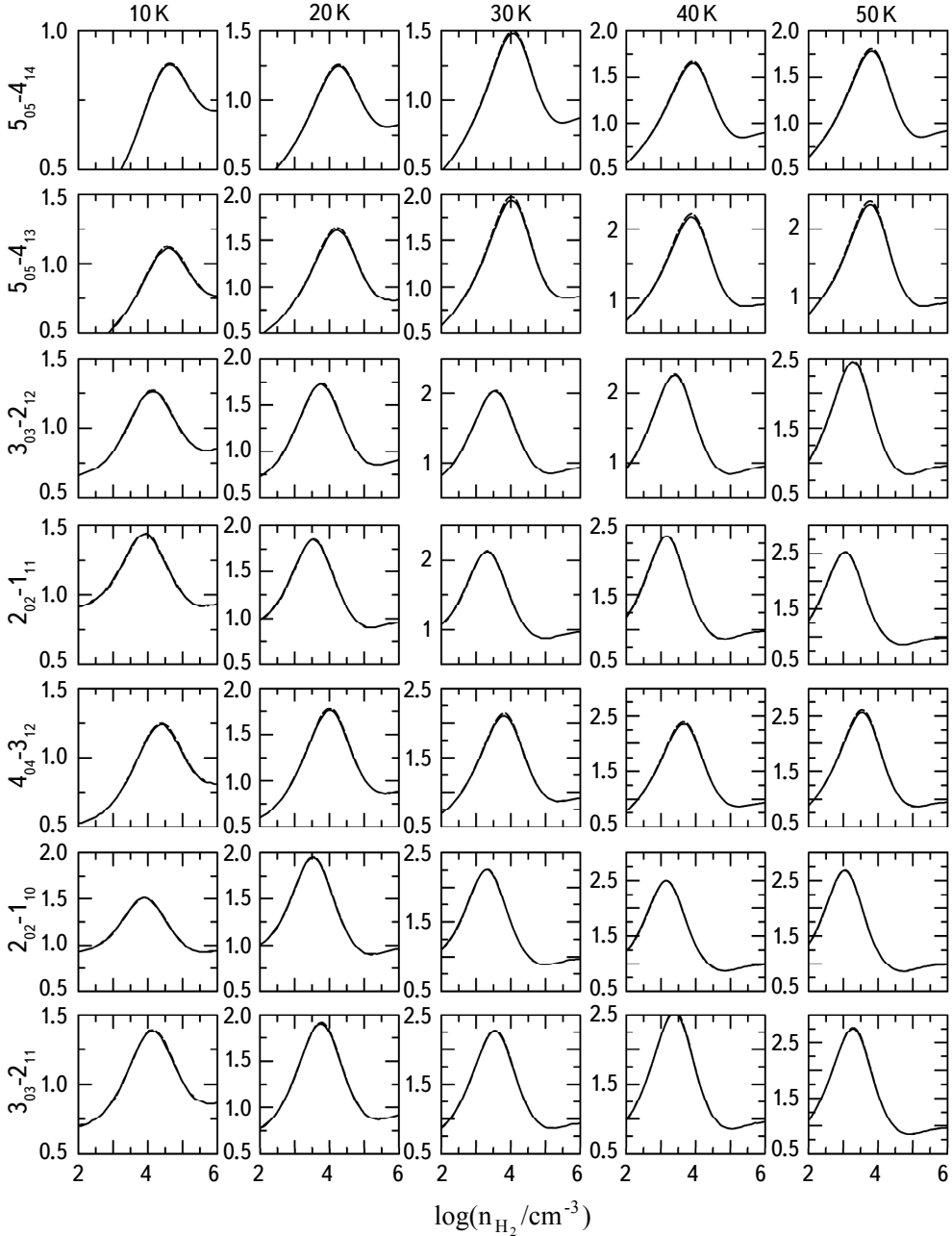


Fig.1. Variation of  $n_u g_l / n_g g_u$  versus molecular hydrogen density  $n_{\text{H}_2}$  for kinetic temperatures of 10, 20, 30, 40 and 50 K, for seven weak MASER transitions of  $\text{NH}_2\text{CH}_2\text{OH}$ , written on the left. Solid line is for  $\gamma = 10^{-5} \text{ cm}^{-3} (\text{km/s})^{-1} \text{ pc}$ , and the dotted line for  $\gamma = 10^{-6} \text{ cm}^{-3} (\text{km/s})^{-1} \text{ pc}$ .

analysis considering all the  $a$ ,  $b$ ,  $c$  type radiative transitions together, for 300 rotational levels of each molecule. Required radiative transition probabilities have

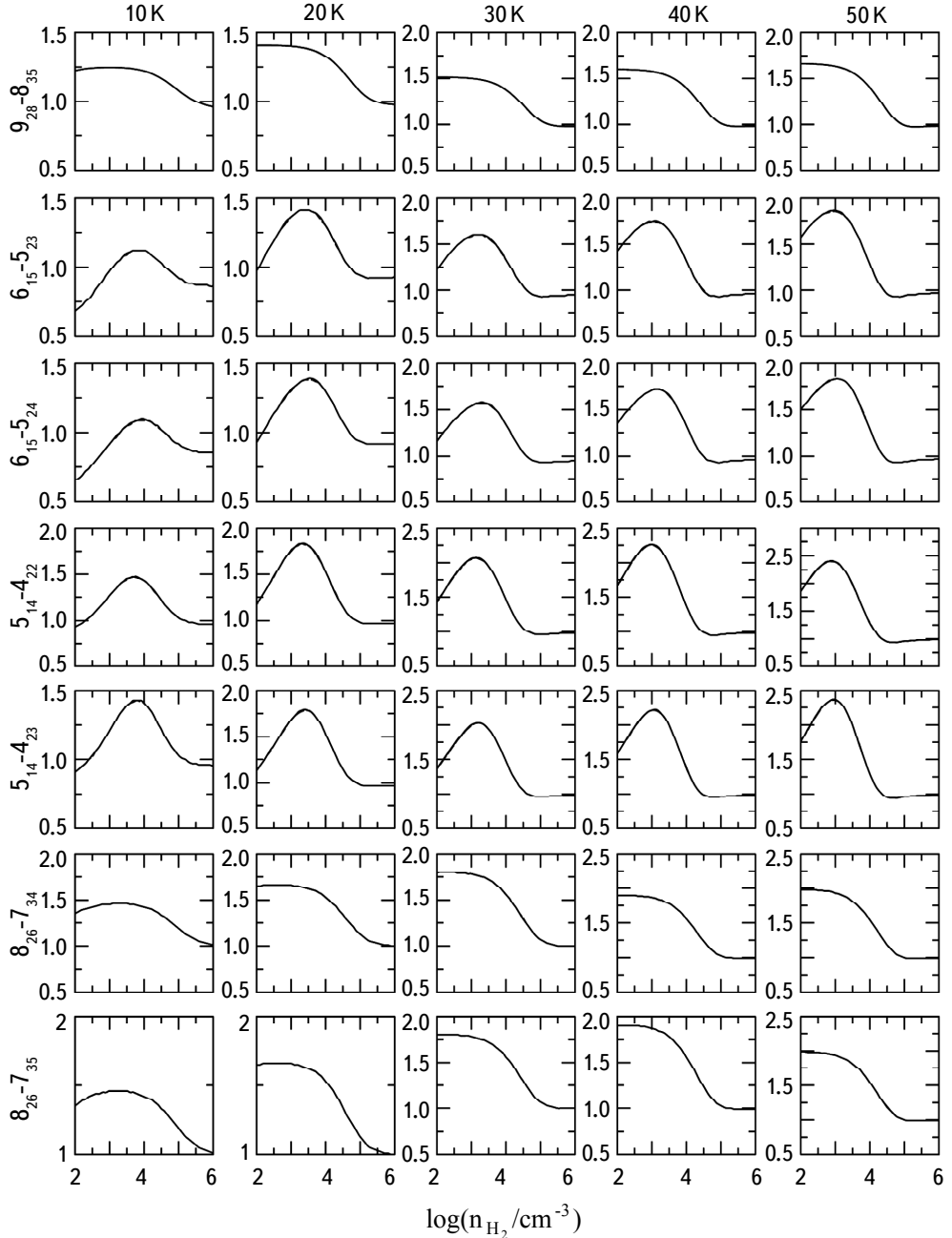


Fig.2. Variation of  $n_{g_i}/n_{g_u}$  versus molecular hydrogen density  $n_{H_2}$ , for kinetic temperatures of 10, 20, 30, 40 and 50 K, for seven weak MASER transitions of  $CH_3NHOH$ , written on the left. Solid line is for  $\gamma = 10^{-5} \text{ cm}^{-3} (\text{km/s})^{-1} \text{ pc}$ , and the dotted line for  $\gamma = 10^{-6} \text{ cm}^{-3} (\text{km/s})^{-1} \text{ pc}$ .

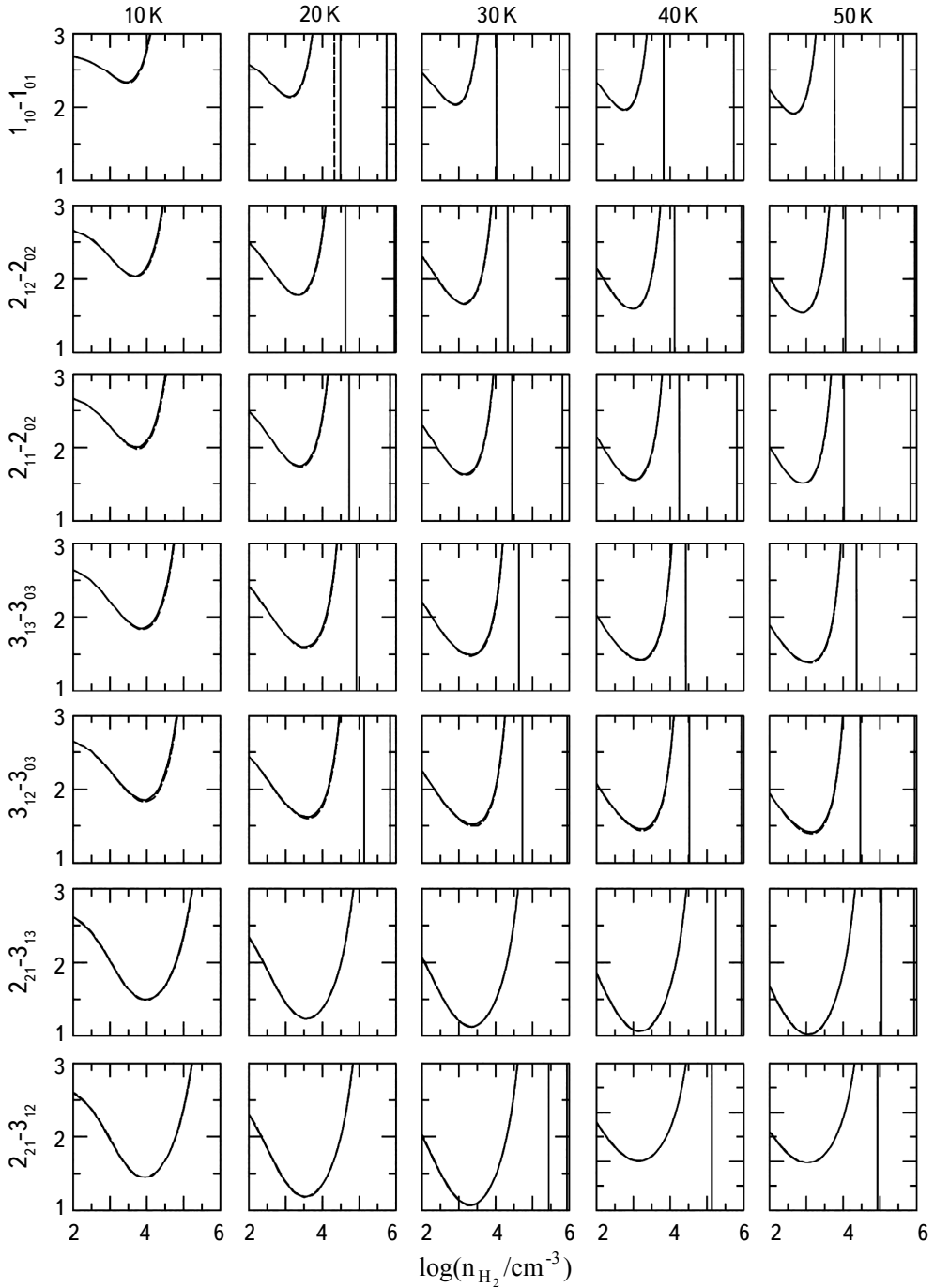


Fig.3. Variation of excitation temperature  $T_{\text{ex}}$  versus molecular hydrogen density  $n_{\text{H}_2}$  for kinetic temperatures of 10, 20, 30, 40, 50 K, for seven anomalous absorption lines of  $\text{NH}_2\text{CH}_2\text{OH}$ , written on the left. Solid line is for  $\gamma = 10^{-5} \text{ cm}^{-3} (\text{km/s})^{-1} \text{ pc}$ , and the dotted line for  $\gamma = 10^{-6} \text{ cm}^{-3} (\text{km/s})^{-1} \text{ pc}$ .

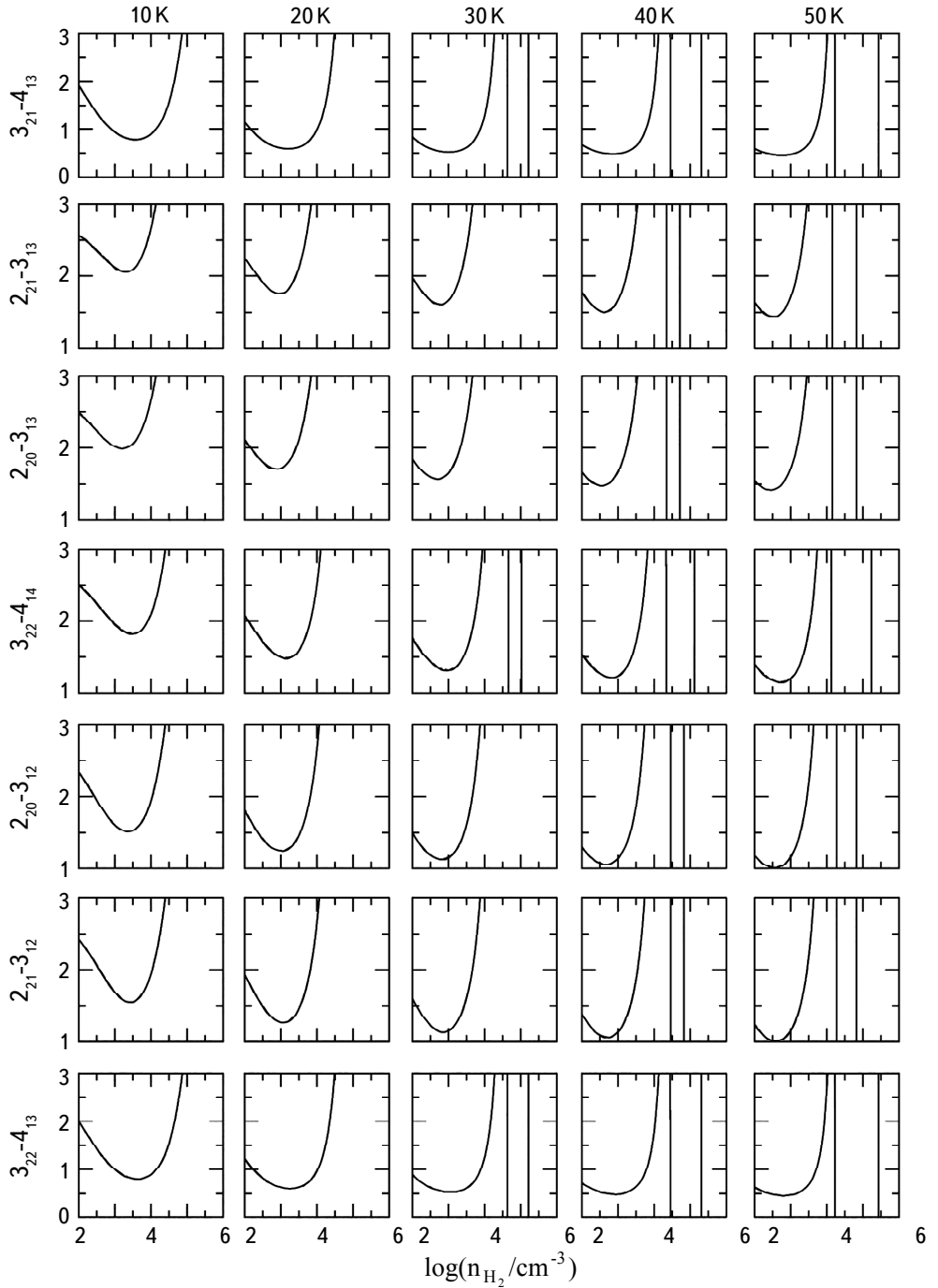


Fig.4. Variation of excitation temperature  $T_{ex}$  versus molecular hydrogen density  $n_{H_2}$  for kinetic temperatures of 10, 20, 30, 40, 50 K, for seven anomalous absorption lines of  $CH_3NH_2OH$ , written on the left. Solid line is for  $\gamma = 10^{-5} \text{ cm}^{-3} (\text{km/s})^{-1}$  and the dotted line for  $\gamma = 10^{-6} \text{ cm}^{-3} (\text{km/s})^{-1}$  pc.

been calculated using the above spectroscopic data. Required collisional rate coefficients have been estimated using a scaling law. The set of statistical equilibrium equations coupled with the equations of radiative transfer is solved through iterative procedure, where initial population densities are taken as the thermal population densities. We have found 181 weak MASERs and 112 anomalous absorption transitions of  $\text{NH}_2\text{CH}_2\text{OH}$ , and 21 weak MASERs and 28 anomalous absorption transitions of  $\text{CH}_3\text{NHOH}$ , which may play important role for the identification of respective molecule in the ISM.

We heartily thank the learned Reviewer for encouraging, constructive and positive comments. MKS is grateful to the authorities of Sunder Deep Group of Institutions. SC is grateful to Hon'ble Dr. Ashok K. Chauhan, Founder President, Hon'ble Dr. Atul Chauhan, Chancellor, Hon'ble Vice Chancellor Dr. Balvinder Shukla, Amity University for valuable support and encouragements.

<sup>1</sup> Physics Department, Sunder Deep Group of Institutions, NH-24, Delhi-Hapur Road, Dasna 201001, India, e-mail: mohitkumarsharma32@yahoo.in

<sup>2</sup> Amity Centre for Astronomy & Astrophysics, Amity Institute of Applied Sciences, Amity University, Sector 125, Noida 201313, U.P., India  
e-mail: schandra2@amity.edu suresh492000@yahoo.co.in

## СОБОЛЕВ LVG АНАЛИЗ АМИНОМЕТАНОЛА И N-МЕТИЛГИДРОКСИЛАМИНА: ПОТЕНЦИАЛЬНЫЕ СПЕКТРАЛЬНЫЕ ЛИНИИ ДЛЯ ИХ ОБНАРУЖЕНИЯ В КОСМИЧЕСКИХ ОБЪЕКТАХ

М.К.ШАРМА<sup>1</sup>, С.ЧАНДРА<sup>2</sup>

Аминометанол ( $\text{NH}_2\text{CH}_2\text{OH}$ ) и N-метилгидроксиламин ( $\text{CH}_3\text{NHOH}$ ) являются изомерами друг друга и имеют астрохимическое значение. Насколько нам известно, они до сих пор не анализировались ни в одной из земных лабораторий и, вероятно, из-за отсутствия точных частот их не искали в космических объектах. Хорошо известно, что физические условия в космических объектах сильно отличаются от условий в земных лабораториях. Следовательно, эти молекулы могут существовать в межзвездной среде. Для получения информации о потенциальных спектральных линиях этих молекул, мы получили их вращательные и центробежные константы дисторсии, а также электрический

дипольный момент с помощью программы GAUSSIAN с использованием метода V3LYP и базисных наборов aug-cc-pVDZ, и aug-cc-pVTZ, отдельно. Поскольку электрический дипольный момент имеет сопоставимые компоненты по всем трем осям  $a$ ,  $b$  и  $c$ , мы рассмотрели все три типа радиационных переходов вместе и рассчитали их вероятность радиационных переходов для всех трех типов. Рассматривая переходы типа  $a$ ,  $b$  и  $c$  вместе, мы выполнили анализ LVG Соболева для каждой молекулы, где коэффициенты скорости столкновений были получены с использованием закона масштабирования. Рассматривая уровни энергии до  $300\text{см}^{-1}$ , мы обнаружили 181 слабую линию MASER и 112 аномальных переходов поглощения  $\text{NH}_2\text{CH}_2\text{OH}$ , а также 21 слабую линию MASER и 28 переходов аномального поглощения  $\text{CH}_3\text{NHOH}$ , которые могут играть важную роль для идентификации соответствующей молекулы в ISM.

Ключевые слова: *ISM: молекулы: аминметанол: перенос излучения*

## REFERENCES

1. *L.Kolesnikova, J.L.Alonso, C.Bermudezet et al.*, *Astron. Astrophys.*, **591**, L5, 2016.
2. *B.M.Hays, S.L.Widicus Weaver*, *J. Phys. Chem.*, **117**, 7142, 2013.
3. *M.N.McCabe, C.R.Powers, B.M.Hays et al.*, 71st International Symposium on Molecular Spectroscopy: June 20-24, at The University of Illinois at Urbana-Champaign, Abstract id.TH08, 2016.
4. *C.Lee, W.Yang, R.G.Parr et al.*, *Phys. Rev.*, **37**, 785, 1988.
5. *A.D.Becke*, *Chem. Phys.*, **98**, 5648, 1993.
6. *Z.Kisiel*, in Demaison J et al. *Spectroscopy from Space*, Kluwer, Dordrecht 91, 2001.
7. *M.Sharma, M.K.Sharma, U.P.Verma et al.*, *Adv. Space Res.*, **54**, 252, 2014a.
8. *M.K.Sharma, M.Sharma, U.P.Verma et al.*, *Adv. Space Res.*, **54**, 1963, 2014b.
9. *M.K.Sharma, M.Sharma, U.P.Verma et al.*, *Adv. Space Res.*, **55**, 434, 2015.
10. *M.K.Sharma, M.Sharma, N.Kumar et al.*, *Ind. J. Phys.*, 2021.
11. *S.Chandra, W.H.Kegel*, *Astron. Astrophys.*, **142**, 113, 2000.
12. *T. de Jong*, *Astron. Astrophys.*, **26**, 297, 1973.
13. *W.H.Kegel*, *Astron. Astrophys. Suppl.*, **38**, 131, 1979.
14. *S.Chandra, S.V.Shinde*, *Astron. Astrophys.*, **423**, 235, 2004.
15. *S.Chandra, P.G.Musrif, S.V.Shinde*, *Bull. Astron. Soc. India*, **34**, 11, 2006.
16. *S.Chandra, S.V.Shinde, W.H.Kegel et al.*, *Astron. Astrophys.*, **467**, 371, 2007.

17. *S.Chandra, A.Kumar, M.K.Sharma*, *New Astron.*, **15**, 318, 2010.
18. *S.Chandra, A.Kumar, B.K.Kumthekar et al.*, *New Astron.*, **16**, 152, 2011.
19. *M.K.Sharma, S.Chandra*, *Ind. J. Phys.*, (under revision), 2021a.
20. *M.K.Sharma, S.Chandra*, *Astrophys. Astron.*, (under revision), 2021b.
21. *E.Rausch, W.H.Kegel, E.Tsuji et al.*, *Astron. Astrophys.*, **315**, 533, 1996.
22. *M.K.Sharma, M.Sharma, S.Chandra*, *Adv. Space Res.*, **62**, 3229, 2018.
23. *M.K.Sharma*, *Astrophys. Astron.*, **40**, 10, 2019a.
24. *M.K.Sharma*, *Mol. Astrophys.*, **15**, 1, 2019a.
25. *M.K.Sharma*, *Ind J. Phys.*, 2019c.
26. *A.V.Nesterenok*, *Mon Not. Roy. Astron. Soc.*, **455**, 3978, 2016.